ELSEVIER

Nuclear Instruments and Methods in Physics Research B 130 (1997) 503–506

NIM B
Beam Interactions with Materials & Atoms

Recent results in ion beam induced charge microscopy: Unconnected junction contrast and an assessment of single contact IBIC

T. Osipowicz [a,*], J.L. Sanchez [a], I. Orlić [a], F. Watt [a], S. Kolachina [b], V.K.S. Ong [b], D.S.H. Chan [b], J.C.H. Phang [b]

[a] *Nuclear Microscopy Group, National University of Singapore, Kent Ridge, Singapore 0511, Singapore*
[b] *Centre for Integrated Circuit Failure Analysis and Reliability, National University of Singapore, Kent Ridge, Singapore 0511, Singapore*

Abstract

The recent development of Ion Beam Induced Charge Microscopy (IBIC) promises to deliver a powerful imaging tool for the analysis of active regions in microelectronics devices. The high penetration power (47 μm for 2 MeV protons in Si) allows direct high resolution access to buried structures, a feature not available to the well established EBIC (Electron Beam Induced Current) technique. As multi-level designs become more prevalent this deep penetration is a significant advantage. We report several results: firstly, that contrast is present in IBIC images from junctions that are not directly connected to the preamplifier. The contrast from unconnected junctions vanishes if these junctions are short circuited. Secondly, we discuss the degradation of IBIC images under prolonged irradiation for protons and He^+ ions. Finally, we discuss the feasibility of single connection IBIC imaging. We demonstrate that IBIC imaging is possible with only one connection to the device substrate. © 1997 Elsevier Science B.V.

1. Introduction

Ion Beam Induced Charge (IBIC) microscopy is a promising tool for the analysis of active regions in semiconductor structures [1,2]. Most work has dealt with the analysis of microelectronics devices. IBIC studies of various ICs [3–5] were carried out. Another application of IBIC is the characterization of field defects and carrier mobility in semiconductor detectors [6].

The analogous electron beam technique (Electron Beam Induced Current, EBIC) is restricted by the limited range of the electron beam to features less than 10 μm deep in Si, while a 2 MeV proton can penetrate as deep as 47 μm. On the other hand, severe beam damage has been found to be a major limitation for the IBIC method [2,7]. The beam damage that causes the reduction of the IBIC charge collection efficiency through the generation of trapping centers is shown here to produce the beneficial side effect of increasing the contrast in the images of device structures when the beam penetrates much deeper than the imaged junction.

From the viewpoint of failure analysis a limitation of IBIC (and EBIC) is that not all junctions can be directly accessed through external pins. Recent ob-

* Corresponding author. Fax: +65-777-6126; email: phyto@leonis.nus.sg

0168-583X/97/$17.00
PII S0168-583X(97)00281-4

servations [8,9] in EBIC analysis with pulsed electron beams have shown that it is possible to image depletion regions that are not directly connected to the preamplifier. The inherently discrete nature of the IBIC pulse generation by individual ions allows the observation of unconnected junctions [10]. A consequence of this result is the possibility to obtain single contact IBIC images as shown in this paper.

2. Experimental procedure

The ion (p or He) beam from the Van de Graaff accelerator is initially focused to produce a beam spot of around 1 μm size. Object and collimator apertures settings are then suitably adjusted to reduce the beam to ~ 1500 ions/s, the current being determined from the count rate of a bright field STIM detector. The device to be imaged is connected to a OMDAQ nuclear electronics data acquisition system with a charge sensitive ORTEC 142A preamplifier. Event by event data acquisition is employed, allowing for off-line data analysis. Images are constructed on-line in map-mode, displaying the intensity of the pulses from a window in the charge collection spectra. However, the best contrast is found to be present in off-line generated images that represent the mean value of the charge collection spectrum for each pixel. All images presented here are obtained with this procedure.

3. Image degradation

The device used was a HCF4007 CMOS transistor array, the design of one of the transistors is shown in Fig. 1. The p-well has a depth of 10 μm and the source and drain regions are 1.2 μm deep. IBIC images were taken with 2 MeV He and 1 MeV p beams. The n-substrate/p-well junction is connected to the preamplifier. Fig. 2a shows the initial IBIC image generated with a 1 MeV proton beam. It can be observed the image is not well resolved. Fig. 2b shows the IBIC image obtained after a total dose of 14.2 protons/μm^2 while Fig. 2c shows both degraded and non-degraded regions. A reduction of the mean charge collection in the degraded region has occurred, and there is also a considerable distortion at the boundary between degraded and nondegraded regions. This arises from an improvement in the image resolution. Fig. 2d shows the image generated using a 2 MeV He beam, showing both the degraded (13.8 protons/μm^2) and non-degraded regions. No significant distortion in features at the boundary between the two regions is observed in Fig. 2d.

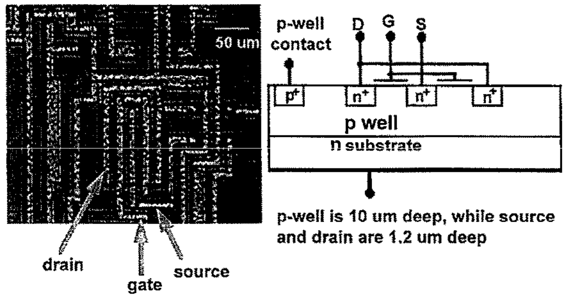

Fig. 1. Optical micrograph of the n-channel transistor. The diagram below represents the available contacts.

Qualitatively, the above behavior can be explained if one considers the large difference of the

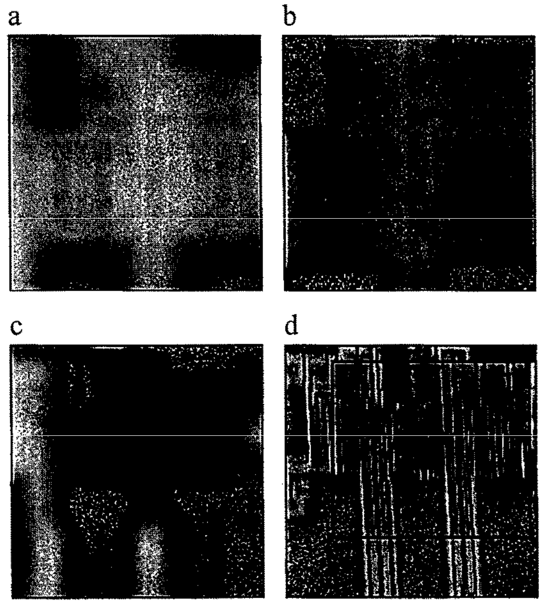

Fig. 2. (a) 1 MeV proton IBIC image (before degradation); (b) after degradation); (c) after (b), with doubled scanzise, showing both degraded and undegraded regions; (d) 2 MeV helium ion IBIC image showing degraded (inside the rectangle) and non-degraded regions.

ranges of the ions used: The penetration depth for 1 MeV protons is 26 μm in Si [12], compared to 7 μm for 2 MeV He ions. Most of the charge carrier generation takes place at the end of the ion range [12,1]. This implies that for the proton beam a part of the generated charge is collected after diffusion from deeper regions, and the isotropic diffusion reduces the resolution in the image. At higher fluences, the structural damage in the sample reduces the diffusion length for the carriers thereby increasing the contrast and reducing the amount of collected charge. In the case of the He ions, most of the charge generation occurs close to the junctions therefore degradation reduces the amount of charge collected without changing the resolution. A quantitative model of this process is being developed in order to find optimal imaging parameters in the presence of degradation.

4. Unconnected junction contrast

The device used here is an array of seven bipolar npn-transistors on a p-type substrate. The schematic lay-out and cross section of one of these transistors is shown in Fig. 3. The collector/substrate junction is 14 μm deep. Electrical contacts to the substrate, collector, base and emitter regions were made through the pins of the package. Fig. 4 shows the charge collection image generated from the collector-substrate junction. The different features in Fig. 4a can be identified by comparison with Fig. 3. The large

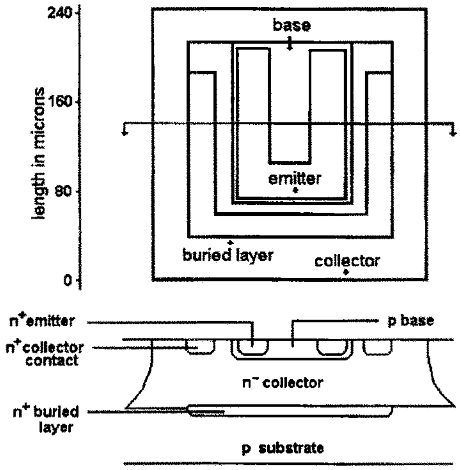

Fig. 3. Schematic layout and cross-section of the transistor.

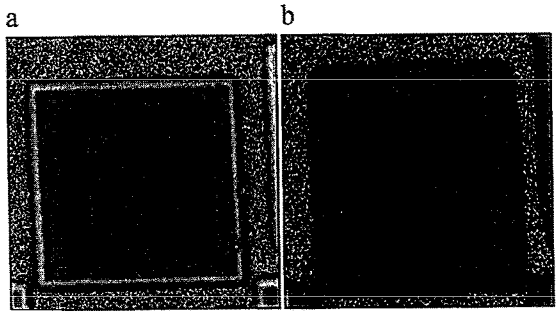

Fig. 4. IBIC images of the collector–substrate junction: (a) with base and emitter floating; (b) with base and emitter shorted.

charge-collection at the edge of the substrate–collector junction produces the bright rim in the figure, and inside this rim the charge collection occurs at the junction between the bottom of the collector and the substrate. The reduced charge collection in the region of the buried layer is due to the small depletion layer width formed by the heavily doped buried layer and the substrate. In the region of the base–collector junction an increased charge collection is visible, and a reduction is seen in the emitter–base junction region. This contrast due to the base–collector and the base–emitter junctions will be referred to as unconnected junction contrast. The contrast due to unconnected junctions vanishes if these junctions are shorted. Fig. 4b shows the IBIC image collected with the unconnected junctions in the transistor under study eliminated by external short. The observation of unconnected junction contrast has been reported and studied in the case of pulsed-EBIC [8]. The signal from the unconnected junctions arises due to the presence of parasitic capacitances between the regions of the device that are floating and the ground plane. A detailed model for this phenomenon can be found in Refs. [8,9].

5. Single contact

The phenomenon of unconnected junction contrast can be utilized to realize a new IBIC imaging mode, Single Contact IBIC. Ong et al. [9] have earlier reported that it is possible to generate single-contact EBIC images. Only one contact to the data acquisition system is made, and all other pins are left floating while the charge collecting circuit is com-

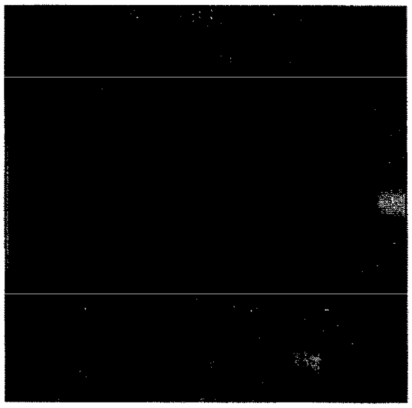

Fig. 5. Single contact IBIC image of the HCF4007 transistor array, substrate connected to preamplifier.

pleted through parasictic capacitances. This charge collection configuration can be applied to IBIC imaging. A HCF4007 CMOS transistor array was used to demonstrate single contact IBIC imaging. Fig. 5 shows an IBIC image generated with only the substrate connected to the preamplifier. It can be seen from Fig. 5 that the various features of the CMOS transistors are visible in the single contact IBIC image despite the fact that there is only a single connection to the preamplifier. This mode of IBIC imaging is very useful in studying complex VLSI circuits where it is not possible to connect all desired junctions to the preamplifier. Another important possibility may be the generation of images from unbonded and unpackaged dies.

6. Conclusion

Both the beam penetration depth and degradation were found to influence IBIC images when the penetration depth is larger than the depth of the depleted region. Significant contrast from unconnected junctions was found in IBIC images. This contrast mechanism was extended to obtain Single Contact IBIC images. These new modes of IBIC are promising tools for the study of microelectronic devices.

References

[1] M.B.H. Breese, J. Appl. Phys. 74 (1993) 3789.
[2] M.B.H. Breese, D.N. Jamieson and P.J.C. King, Materials Analysis Using a Nuclear Microprobe (Wiley, New York, 1996).
[3] F.W. Sexton, K.M. Horn, B.L. Doyle, J.S. Laird, M. Cholewa, A. Saint, G.J. Legge, Nucl. Instr. and Meth. B 79 (1993) 436.
[4] M. Takai, Nucl. Instr. and Meth. B 113 (1996) 330.
[5] M.B.H. Breese, P.J.C. King, G.W. Grime, F. Watt, J. Appl. Phys. 72 (1992) 2097.
[6] M. Jacsic, I. Bogdanovic, M. Bogovac, S. Fazinic, S. Galassini, K. Kovacevic, C. Manfredotti and E. Vittone, Nucl. Instr. and Meth. B 113 (1996) 378.
[7] M.B.H. Breese, C.H. Sow, D.N. Jamieson, F. Watt, Nucl. Instr. and Meth. B 85 (1994) 790.
[8] V.K.S. Ong, D.S.H. Chan and J.C.H. Phang, 4th Int. Symp. on the Physical and Failure Analysis of Integrated Circuits, Singapore, eds. Y.K. Swee, S.H. Ong and D.S.H. Chan (IEEE, Singapore, 1993) p. 45.
[9] V.K.S. Ong, An investigation into the Electron Beam Induced Current effects on semiconductor materials and devices, Ph.D. thesis, National University of Singapore, Singapore (1996).
[10] S. Kolachina, V.K.S. Ong, D.S.H. Chan, J.C.H. Phang, T. Osipowicz, F. Watt, Appl. Phys. Lett. 68 (1996) 532.
[11] F. Watt, I. Orlic, K.K. Loh, C.H. Sow, P. Thong, S.C. Liew, T. Osipowicz, T.F. Choo, S.M. Tang, Nucl. Instr. and Meth. B 85 (1994) 708.
[12] J.F. Ziegler, J.P. Biersack and U. Littmark, The Stopping and Range of Ions in Solids (Pergamon, New York, 1985).